

Dynamic Object Localization via a Proximity Sensor Network

G. Petryk and M. Buehler

Department of Mechanical Engineering
Centre for Intelligent Machines, McGill University
Montréal, QC H3A 2A7, CANADA

Abstract

In this paper we describe a Proximity Sensor Network (PSN) consisting solely of inexpensive intensity-based electro-optical proximity sensors embedded in a robotic end-effector. By coupling the PSN to an extended Kalman filter, and by resolving the sensors' dependence on ambient light, the object's reflective properties, and the angle between sensor beam and the object's surface, we succeed in estimating a cylindrical moving object's unknown planar trajectory. Experiments show robust position and velocity estimation of the moving object, despite noisy sensor data and unmodelled object dynamics. Such a system should be directly applicable to sensor-based control approaches for dynamic grasping and manipulation in robotics and automation.

1 Introduction

Autonomous grasping of objects with known geometry but unknown or uncertain motion is a common and important problem in robotics and automation. Past research in this area has focused on sensing, planning, or integrated, sensor-based control approaches. This paper falls into the first category, and addresses new issues in sensing and sensor fusion for autonomous grasping.

For purposes of object tracking, cameras are most versatile. However, when used in close proximity to objects in grasping tasks, cameras can encounter problems with lighting, focusing, sensing bandwidth, size, and occlusion. Lighting, focusing, and occlusion problems are most severe at the most inopportune time – when the object is close to the end-effector just prior to contact.

Most of these problems can be remedied by active electro-optical proximity sensors which have a long history in the robotics research community [3, 5]. These devices work in the infra-red spectrum and are based on three different operating principles. *Triangulation*-based sensors tend to be the most accurate, but due to geometric constraints, tend to be almost as large as miniature cameras and have limited close range [7, 14]. Masuda [12] uses the *phase shift* of the received signal to measure distance, angle or orientation depending on the mode of

operation. The sensor consists of six LEDs in a cross shaped pattern with the photo transistor in the center. Goldenberg et al. [13] show how this sensor's design parameters affect its performance and propose an optimal sensor design. The major drawback of this approach is the required base line separation of the sensors of several centimeters, and the costly processing electronics.

For these reasons, *intensity-based* electro-optical proximity sensors are most commonly proposed for close range sensing. However, they come with their own set of challenges. The sensor signal depends not only on distance, but also on ambient light, the object's reflective properties, and the angle between sensor beam and the object's surface. Previous research proposed solutions to subsets of the problems – by assuming a negligible angle dependence and known reflective properties [9], unknown reflective properties and known object motion [4, 10] and known reflective properties and unknown motion [1]. The simplifying assumptions in [10] allow a simple two parameter extended Kalman filter to be used since only the sensor to target distance and surface parameters need be estimated. In addition, only the perpendicular distance is estimated thus eliminating the need for concurrent estimation of target surface angle. For the situation where several distances are used to recover target attitude, a separate filter for each sensor had to be maintained.

In this paper, we propose a solution for estimating the unknown planar motion as well as the surface reflective properties of a maneuvering target. This is possible by assuming a known object geometry, and using this information for sensor fusion of several sensor outputs via an extended Kalman filter. The assumption of known object geometry is reasonable in many practical situations, where at least an approximate object model is available. This framework permits the simultaneous estimation of the object's reflectance properties, allows for angle dependent sensor models, all while tracking an unknown object trajectory.

The paper is organized as follows. Sec. 2 introduces the PSN and its sensors. Sec. 3 describes the PSN sensor fusion via an extended Kalman filter, and the object model and any simplifying assumptions. The experimental results are shown and analyzed in Sec. 4.

2 Proximity Sensor Network

2.1 Sensor Hardware

The infra-red sensors used are STMTM proximity sensors. The sensor heads are cylinders 5mm in diameter and 13mm in length. A cable extends from the heads to a proprietary amplifier package. The output of the amplifier is an analog signal which ranges from 0 to 2.7V . This signal was sampled by a Transputer-based [11] real-time data acquisition system. The maximum range of the sensors was approximately 80mm .

2.2 Sensor Characterization

The output voltage of an active infra-red sensor was assumed to be dependent on three parameters: sensor-target distance, d , sensor-target angle θ , and the target’s reflectance properties, λ . Object features were assumed to be large compared to the sensors and thus the effect of local surface curvature was neglected.

The sensors were characterized by experiment: sensor output voltage was recorded while a flat plane covered with white paper was placed at distance intervals of 1mm and orientation intervals of 1.5° over a range of $0-75\text{mm}$ and -50° to $+50^\circ$, respectively. The sensor saturated at distances less than 5mm when the orientation was less than $\pm 30^\circ$. This region was avoided for the rest of the characterization.

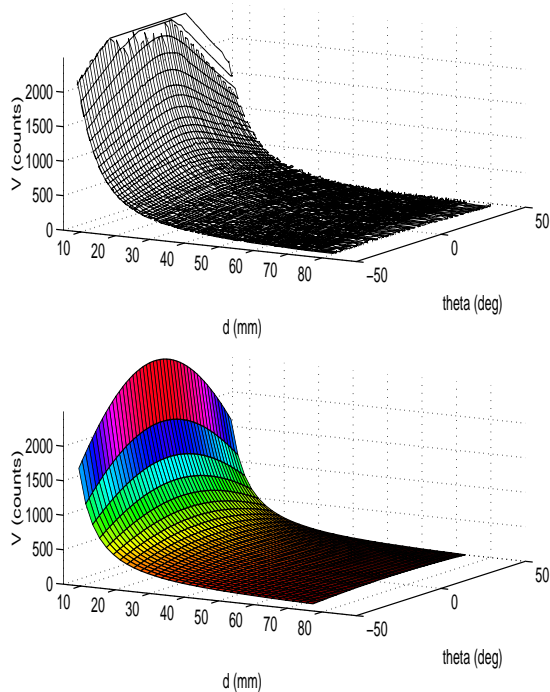


Figure 1: *Top: Raw sensor data, Bottom: Surface plot of characterized sensor data. Voltage units are analog to digital (A/D) converter counts.*

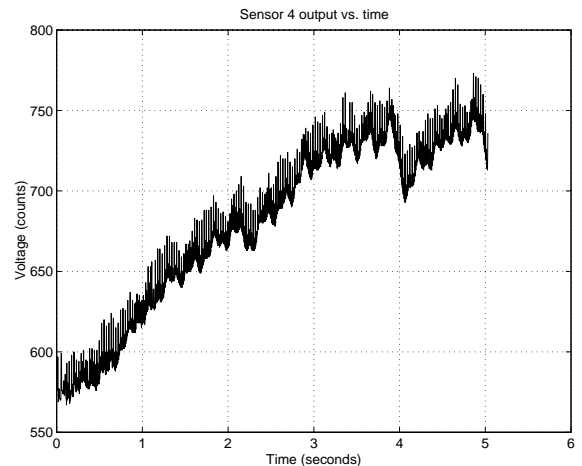


Figure 2: *Typical proximity sensor data.*

The relationship between sensor output, h , (which is proportional to the intensity of the received infra-red light reflected by the object) and sensor-target distance, d , is the well known inverse square law [4, 8, 10]. The angle dependence relationship was obtained by assuming the object’s surface was Lambertian [6, 8]. Finally, the surface properties of the object (color, texture, finish) were lumped into a single “reflectance gain”, λ , as in [4, 10]. The sensor model used was therefore

$$h(d, \theta, \lambda) = \frac{\lambda\beta_1}{d^{\beta_2}} \cos(\beta_3\theta). \quad (1)$$

The sensor model would be greatly simplified if there were no angle dependence. While some previous research (e.g. [10]) assumes that surface angle dependence is negligible, Fig. 1 shows that this was not the case with our sensors. These findings agree with the theoretical development found in [4].

The parameters β_j were determined by fitting (1) to experimental data using recursive least squares (RLS). The raw data and fitted data surfaces are both shown in Fig. 1. The relation fit the data with a root mean square (RMS) error of less than 2%. The sensor noise variance was computed as approximately 60 A/D counts from the output of a sensor aimed at a stationary flat surface. Since the output curve’s gradient in any direction is small for large sensor-target distances, noise limits the maximum useful range of the sensor. A typical sensor output is shown in Fig. 2.

3 Data Fusion

3.1 Extended Kalman Filtering

Measurements from the PSN sensors are non-linear, noisy, and configuration dependent. In addition, autonomous grasping requires real-time identification of the

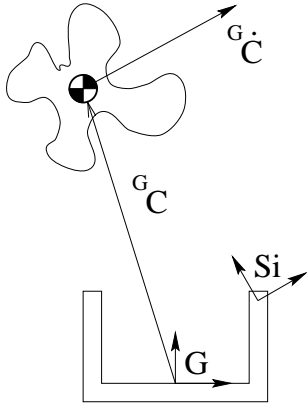


Figure 3: *PSN sensing an arbitrary object. Position, C , and velocity, \dot{C} , are estimated with respect to gripper-local coordinates, G , but transformed to each of the i sensor-local coordinates, S_i , when evaluating the measurement equation $h(x)$.*

parameter and state. For these reasons, an extended Kalman filter (EKF) with linearization of the observation equation was selected to perform data fusion for the PSN.

A PSN sensing an arbitrary object is shown in Fig. 3. The object is modelled as free-flying with no external forces, treating any accelerations as disturbances. Its kinematic states are position and velocity of its center of mass. The object's reflectance gain, λ , is adjoined to the kinematic state vector so that it may be estimated simultaneously. The discrete state equation is therefore

$$x_{k+1} = \Phi x_k + w_k \quad (2)$$

where,

$$x_k = [C_x, \dot{C}_x, C_y, \dot{C}_y, \lambda]^T, \quad (3)$$

$$\Phi = \begin{pmatrix} \xi & 0_{2 \times 2} & 0_{2 \times 1} \\ 0_{2 \times 2} & \xi & 0_{2 \times 1} \\ 0_{1 \times 2} & 0_{1 \times 2} & 1 \end{pmatrix}, \quad (4)$$

$$\xi = \begin{pmatrix} 1 & \tau \\ 0 & 1 \end{pmatrix}, \quad (5)$$

and τ is the sampling period. The system is observed with the measurement equation

$$y_k = h(x_k) + v_k, \quad (6)$$

where h is the sensor model described in Sec. 2.2.

The noise processes were assumed to have the following statistics:

$$E[v_k v_l] \approx R \delta_{kl} \quad (7)$$

$$E[w_k w_l] \approx Q \delta_{kl} \quad (8)$$

where E is the statistical expected value function. The state error covariance matrix, Q , and sensor noise covariance matrix, R , are assumed constant.

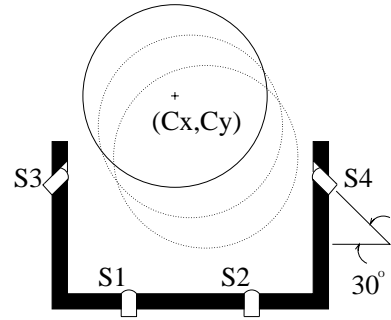


Figure 4: *PSN sensing a circular object.*

The parameters are estimated using an extended Kalman filter. The EKF equations are:

Prediction

$$x_{k+1|k} = \Phi x_k \quad (9)$$

$$P_{k+1|k} = \Phi P_k \Phi^T + Q \quad (10)$$

Update

$$x_{k+1|k+1} = x_{k+1|k} + K[y_{meas,k+1} - h(x_{k+1|k})] \quad (11)$$

$$P_{k+1|k+1} = S P_{k+1|k} S^T + K R K^T \quad (12)$$

where,

$$S = [I - K H_{k+1}], \quad (13)$$

the Kalman gain is defined as,

$$K = P_{k|k-1} H_k^T [H_k P_{k|k-1} H_k^T + R]^{-1}, \quad (14)$$

the Jacobian as,

$$H_k = \left[\frac{\partial h(x)}{\partial x} \right]_{x=x_{k+1|k}} \quad (15)$$

and P is the covariance matrix. Any known sensor displacement, for example due to robot motion, would be added to the RHS of (2) and therefore (9).

3.2 Simulations

Given a proper measurement equation, $h(x)$ and its Jacobian, H , the EKF described above may be used to estimate the pose of any object. Simulations of a two dimensional PSN and its EKF estimating the location of a circle were conducted. The PSN was composed of four sensors arrayed as shown in Fig. 4.

The only complication in applying the filter equations is evaluating the measurement equation for each sensor. Prior to evaluation, the state variables must be transformed from end-effector-fixed coordinates to sensor-local coordinates. This is accomplished using the transformation matrix

$${}^{S_i}T_G = \begin{bmatrix} \cos \alpha_i & -\sin \alpha_i & S i_x \\ \sin \alpha_i & \cos \alpha_i & S i_y \\ 0 & 0 & 1 \end{bmatrix} \quad (16)$$

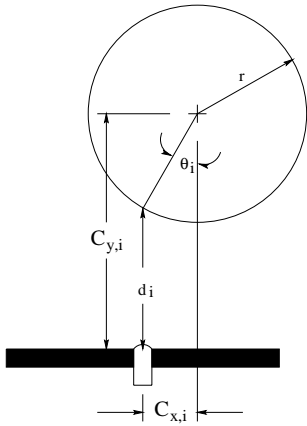


Figure 5: *Sensor-local variable assignments.*

where α_i is the angle between the x-axis of the end-effector and sensor coordinate systems, and S_{i_x}, S_{i_y} are the components of the distance between the origins of the two coordinate systems.

The transformed state vector is then used to calculate the sensor model's variables, d and θ . The reflectance gain, λ , is invariant to this transformation. The relation between d , θ , and the state variables for the i^{th} sensor is shown in Fig. 5 and is described by

$$\theta_i = \text{asin}\left(\frac{x_i}{r}\right) \quad (17)$$

$$d_i = y_i - r \cos(\theta_i). \quad (18)$$

A number of simulations were run with various initial conditions, measurement noise levels, modelling errors, sensor positions and number of sensors. From these simulations it was observed that the filter worked well when the object was in view of all four sensors of the PSN. However, there were situations, such as improper tuning of the Q matrix, inadequate initial conditions or when the object was in sight of less than four sensors, in which the filter would diverge. Thus in practice, a supervisory level should be implemented to detect filter divergence and reset the filter.

4 Experiments

The experiments were conducted on a planar robotic testbed. The robot is a PPR (prismatic-prismatic-revolute) manipulator with a dextrous workspace [2] of 600mm x 300mm. Control and data acquisition for the PPR robot was done via a two node INMOS© transputer network. Sampling and servoing were done at rate of 300Hz.

The simulation situation was reproduced experimentally to test the PSN with real data. A cylinder 65mm in diameter wrapped in white paper was moved with constant velocity on the PPR robot in front of a stationary

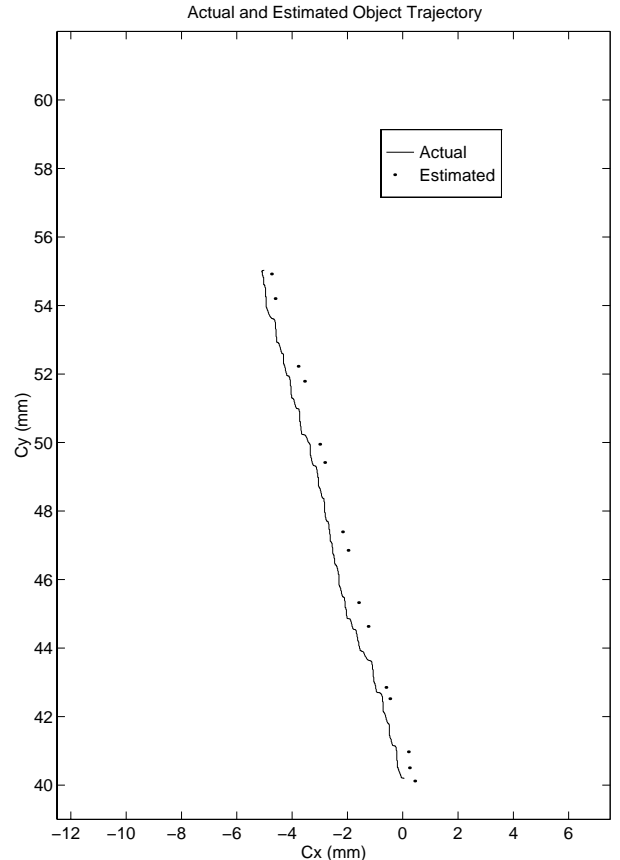


Figure 6: *PSN Tracking a cylindrical object moving with constant velocity.*

PSN arrayed as shown in Fig. 4. The sensors were recessed from the gripper surface so as to avoid the region in which they saturate. The EKF was initialized with $Q = \text{diag} [0.001, 0.01, 0.001, 0.01, 0.01]$, $P = I$ and R equal to the identity matrix multiplied by the sensors experimental variance value of 60. Initial values of the states were equal to 50% of their actual values.

The experimental results were very good. Fig. 6 shows a comparison between the actual and the estimated planar position of the moving object, when given a large initial estimation error. A more detailed look at convergence and tracking is provided in Fig. 7, which shows the errors in all four states and the reflectance gain over time. Initial error transients disappear within 0.3 seconds, and remain small thereafter. In particular, the position estimation accuracy is better than 1 mm. The state errors never converge exactly to zero in part because the object experienced unmodelled accelerations throughout the experiment as evident from Fig. 6.

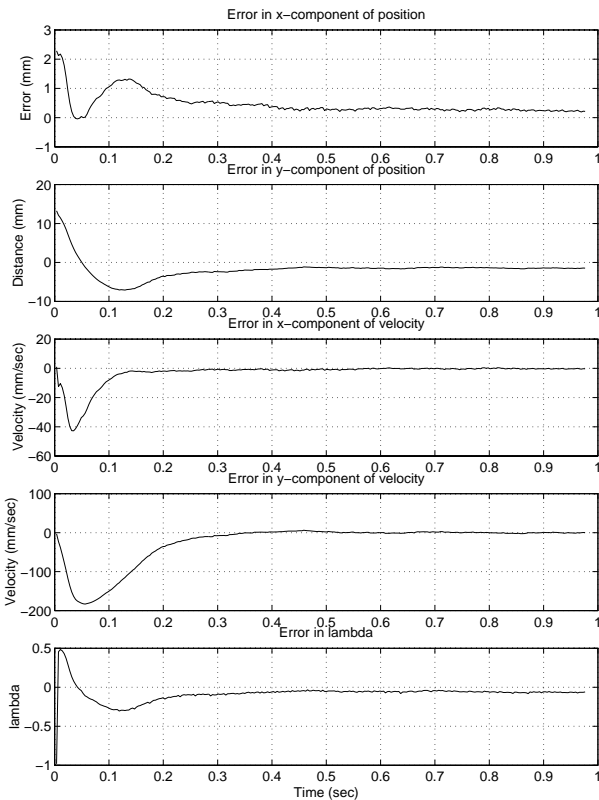


Figure 7: PSN tracking errors for each of the five states.

5 Conclusions

We have described a Proximity Sensor Network (PSN) with intensity-based electro-optical proximity sensors. By assuming a known object geometry, and using this information for sensor fusion of several sensor outputs via an extended Kalman filter, this framework permits the simultaneous estimation of the object's reflectance properties, allows for angle dependent sensor models, all while tracking an object's trajectory. Experiments show robust position and velocity estimation of the moving object, despite noisy sensor data and unmodelled object dynamics. The resulting system will be used for sensor-based control of dynamic grasping and manipulation in robotics and automation.

Acknowledgements

Support for this research was provided in part by the Institute for Robotics and Intelligent Systems (IRIS), a federally-funded Network of Centers of Excellence. Support for GP was provided by Québec's Fonds pour la Formation de Chercheurs et l'Aide à la Recherche (FCAR). The authors would like to thank J. Damianakis for his help in setting up the experimental testbed used for this research.

References

- [1] E. Cheung and V. Lumelsky. Development of sensitive skin for a 3d robot arm operating in an uncertain environment. In *Proc. IEEE Int. Conf. Robotics and Automation*, pages 1056–1061, Piscataway, NJ, 1989.
- [2] J.J. Craig. *Introduction to Robotics Mechanics and Control*. Addison Wesley, Reading, MA, 1986.
- [3] H.A. Ernst. *MH-1, a computer-operated mechanical hand*. PhD thesis, M.I.T., Dec 1961.
- [4] B. Espiau and J.Y. Catros. Use of optical reflectance sensors in robotics applications. *IEEE Trans. Systems, Man, and Cybernetics*, 10(12):903–912, Dec 1980.
- [5] A.R. Johnston. Proximity sensing technology for manipulator end effectors. *Mechanism and Machine Theory*, 12:95–109, 1977.
- [6] S.M. Juds. *Photoelectric Sensors and Controls*. Marcel Dekker, Inc., NY, 1988.
- [7] L. Korba, S. Elgazzar, and T. Welch. Active infrared sensors for mobile robots. *IEEE Trans. Instrumentation and Measurement*, 43(2):283–7, Apr 1994.
- [8] M. D. Levine. *Vision in Man and Machine*. McGraw Hill, Montreal, 1985.
- [9] Y.F. Li. Robot end-effector orientation control using proximity sensors. *Robotics and Computer-Integrated Manufacturing*, 10(5):323–331, 1993.
- [10] Y.F. Li. Characteristics and signal processing of a proximity sensor. *Robotica*, 12:335–41, 1994.
- [11] INMOS Limited. *IMS T805 transputer*. Bristol, U.K., 1988.
- [12] R. Masuda. Multifunctional optical proximity sensor using phase modulation. *J. Robotic Systems*, 3(2):137–147, 1986.
- [13] O. Partaatmadja, B. Benhabib, and A. Goldenberg. Analysis and design of a robotic distance sensor. *J. Robotic Systems*, 10(4):427–445, 1993.
- [14] G. Skofte and G. Hirzinger. Computing position and orientation of a freeflying polyhedron from 3d data. *Proc. IEEE Int. Conf. Robotics and Automation*, pages 150–155, Apr 1991.